COMM. MATH. SCI.
Vol. 1, No. 2, pp. 377–384

HIGHER ORDER STRING METHOD FOR FINDING MINIMUM ENERGY PATHS*

WEIQING REN†

Abstract. The string method is an efficient numerical method for finding transition paths and transition rates in metastable systems. The dynamics of the string are governed by a Hamilton-Jacobi type of equation. We construct a stable and high order numerical scheme to estimate the first order spatial derivatives, or the tangent vectors in the equation. The construction is based on the idea of the upwind scheme and the essentially nonoscillatory scheme (ENO). Numerical examples demonstrate the improvement of the accuracy by the new scheme.

1. Introduction

The string method is an efficient numerical method for finding transition pathways and transition rates in metastable systems [2][3][4][12]. It has two versions. The zero-temperature version is designed for smooth energy landscapes, and the finite-temperature version is designed for rough energy landscapes, in which case thermal noise acts to smooth out the small scale features. In this paper, we shall focus on the zero-temperature string method and design a stable numerical scheme which achieves higher order accuracy. The basic idea of the string method is to represent transition paths by curves with intrinsic parameterizations. Such curves are called strings. The strings are evolved by the the potential force in the normal directions, and converge to an invariant manifold of the deterministic dynamics of the gradient system, which is known as the minimum energy path (MEP). The MEP gives the optimal transition path in the zero-temperature limit. The potential energy barrier ΔV can be obtained from the MEP and to leading order the transition rate is given by $\exp(-\frac{\Delta V}{\varepsilon})$, where ε is a small parameter proportional to the temperature.

The dynamics of the string are governed by a first order Hamilton-Jacobi type of equation. The approximation to the spatial derivative, or the tangent vector of the string, has to be carefully done in order to avoid numerical instabilities. For example, if central finite difference is used to estimate the tangent vectors, kinks will form in regions where the parallel component of the potential force is large compared with the perpendicular component [6]. One remedy to this problem is to use one-side biased finite difference, or the upwind scheme, based on the energy profile along the path. However, the upwind scheme is only first order accurate and it leads to poor accuracy, especially in regions where the path is curved. The error will be magnified significantly when calculating the transition rates.

The aim of this paper is to construct a stable and higher order numerical scheme for the string method. We shall briefly introduce the (zero-temperature) string method in section 2. Then in section 3, we construct the higher order scheme by combining the idea of the upwind scheme with the essentially nonoscillatory scheme (ENO). We test the accuracy of the new scheme in section 4, and conclusion remarks are made in section 5.

2. String Method

In this section, we describe the string method for the calculation of minimum energy paths for smooth energy landscapes. Let us consider the system modeled by

* Received: December 23, 2002; accepted: Janurary 7, 2003.
† School of Mathematics, Institute for Advanced Study, 1 Einstein Drive, Princeton, New Jersey 08540

the Langevin equation:

$$\dot{X}^\varepsilon = -\nabla V(X^\varepsilon) + \sqrt{2\varepsilon}\dot{W}. \tag{2.1}$$

We assume $V(x)$ has at least two minima a and b, and we look for the MEP between them.

Let φ be a curve connecting a and b. A simple way to find the MEP is to evolve φ according to the velocity given by

$$u = -(\nabla V)^\perp(\varphi), \tag{2.2}$$

where $(\cdot)^\perp$ denotes the projection of $(\cdot)$ into the hyperplane normal to φ. The stationary solution of (2.2) satisfies

$$(\nabla V)^\perp(\varphi) = 0, \tag{2.3}$$

which defines the MEP of V.

For the purpose of numerical simulation, it is convenient to have an evolutionary equation for the curve. Let $\varphi(\alpha, t)$ be the instantaneous position of the string which is parameterized by α. Then we can rewrite (2.2) as

$$\varphi_t = -(\nabla V)^\perp(\varphi) + r\hat{t} \tag{2.4}$$

where

$$(\nabla V)^\perp = \nabla V - (\nabla V, \hat{t})\hat{t}, \tag{2.5}$$

and $\hat{t}$ is the unit tangent vector of φ:

$$\hat{t} = \frac{\varphi_\alpha}{|\varphi_\alpha|}. \tag{2.6}$$

The scalar field $r(\alpha, t)$ is a Lagrange multiplier which is uniquely determined by the parameterization of φ. In the simplest case when φ is parameterized by its normalized arclength so that $\varphi(0) = a$ and $\varphi(1) = b$, we need

$$\frac{\partial}{\partial\alpha}|\varphi_\alpha| = 0 \tag{2.7}$$

which gives

$$r(\alpha, t) = \alpha \int_0^1 (\nabla V, \hat{t}_{\alpha'})d\alpha' - \int_0^\alpha (\nabla V, \hat{t}_{\alpha'})d\alpha'. \tag{2.8}$$

Other parameterization, for example, by energy weighted arclength which increases the resolution at the transition state, can be implemented as well by modifying the constraints (2.7). We call such curves with intrinsic parameterizations strings.

In practice, (2.4) is solved by a time-splitting scheme. The strings are discretized into a collection of points. These points are evolved by solving

$$\varphi_t = -(\nabla V)^\perp(\varphi) \tag{2.9}$$

using standard ODE solvers, such as the forward Euler method, or the TVD Runge-kuta method. A reparameterization step is applied once in a while to enforce the proper parameterization of the strings.

The first order equation (2.9) is a Hamilton-Jacobi type of equation. The approximation to the first order spatial derivative, or the tangent vector, has to be carefully done in order to avoid numerical instabilities. The simplest way to approximate the derivative is to use central finite difference which is second order accurate. Unfortunately, it is unstable and usually develops kinks in regions where the component of the potential force parallel to the MEP is large compared with the perpendicular component. An example of the instability is shown in Figure 4.1.

The numerical instability can be avoided by using one-side biased numerical schemes. We rewrite (2.9) as

$$\varphi_t = \frac{c(\varphi)}{|\varphi_\alpha|}\varphi_\alpha - \nabla V(\varphi), \tag{2.10}$$

where $c(\varphi) = (\nabla V(\varphi), \hat{t})$ is the directional derivative of the potential V along the string $\varphi(\alpha)$. The equation (2.10) suggests an upwind scheme based on the sign of $c(\varphi)$. Specifically, we define

$$\varphi_\alpha(\alpha_i, t) = \begin{cases} \varphi_i^+(t), & \text{if } V(\varphi_{i+1}) > V(\varphi_i) > V(\varphi_{i-1}) \\ \varphi_i^-(t), & \text{if } V(\varphi_{i+1}) < V(\varphi_i) < V(\varphi_{i-1}). \end{cases} \tag{2.11}$$

where

$$\varphi_i^+(t) = \frac{1}{\Delta\alpha}(\varphi_{i+1}(t) - \varphi_i(t)), \quad \varphi_i^-(t) = \frac{1}{\Delta\alpha}(\varphi_i(t) - \varphi_{i-1}(t)). \tag{2.12}$$

If $V(\varphi)$ achieves local minimum or maximum at φ_i, the tangent may be approximated by the potential weighted finite differences, which avoids an abrupt change of the tangent vector [6].

The upwind scheme given by (2.11) and (2.12) is only first-order accurate. Our numerical experiments show that it usually leads to corner cutting of the path when the path is curved, and consequently leads to a over-estimate of the energy barrier. In order to achieve higher order accuracy, a higher order numerical scheme for (2.4) is needed. In the next section, we combine the idea of the upwind scheme and the ENO scheme and construct a numerical scheme which is stable and achieves higher order accuracy.

3. Higher Order String Method

$\varphi_i^\pm$ in (2.11) in general are vectors in high dimensional space. We denote one component of $\varphi_i^\pm$ by $f_i^\pm$ and describe a r-th order ENO scheme for the calculation of $f_i^\pm$ in the following.

ENO schemes have been very successful in solving hyperbolic conservation laws which develop singular solutions, for example, shock waves. It was generalized to Hamilton-Jacobi type of equations in [11] and [9], based on the close connection between the two types of equations. The basic idea of the ENO scheme is to adaptively choose stencils from smooth regions to interpolate the original function, and hence yields a uniformally high order essentially nonoscillatory approximations for piecewise smooth functions. Which stencil to choose depends on some smoothness measurements of the function, for example, the Newton divided differences as described below.

Suppose we are given a collection of function values $\{f_i, i = 0, \pm1, \pm2, \cdots\}$, at discrete nodes $\{\alpha_i\}$. The following algorithm inductively constructs a r-th order polynomial $P^r_{i+\frac{1}{2}}(\alpha)$ to approximate $f(\alpha)$ on the interval $[\alpha_i, \alpha_{i+1}]$. The interpolation

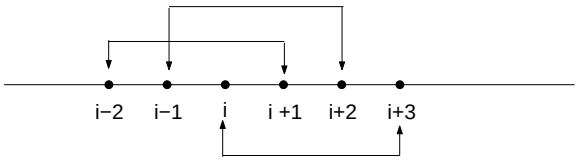

FIG. 3.1. *The three possible stencils for the calculation of f_i^+ with $r = 3$. Algorithm 3.1 chooses one of these based on the local smoothness of the function.*

adaptively choose the neighboring nodes based on the smoothness of the function measured by the Newton divided differences defined inductively by

$$f[\alpha_i] = f_i,$$

$$f[\alpha_i, \alpha_{i+1}, \cdots, \alpha_{i+m}] = \frac{f[\alpha_{i+1}, \cdots, \alpha_{i+m}] - f[\alpha_i, \cdots, \alpha_{i+m-1}]}{\alpha_{i+m} - \alpha_i}.$$

The derivative of $P^{(r)}_{i+\frac{1}{2}}(\alpha)$ at α_i is defined as the right-side biased approximation f_i^+ to the derivative of $f(\alpha)$.

ALGORITHM 3.1. *[r-th order ENO scheme for f_i^+]*

Given $\{f_j, j = 0, \pm 1, \cdots\}$ and i;

$P^{(1)}_{i+\frac{1}{2}}(\alpha) := f[\alpha_i] + f[\alpha_i, \alpha_{i+1}](\alpha - \alpha_i)$;

$k^{(1)}_{\min} := i$;

for $l = 2, 3, \cdots, r$

  $a := f[\alpha_{k^{(l-1)}_{\min}}, \cdots, \alpha_{k^{(l-1)}_{\min}+l}]$;

  $b := f[\alpha_{k^{(l-1)}_{\min}-1}, \cdots, \alpha_{k^{(l-1)}_{\min}+l-1}]$;

  if $|a| \geq |b|$

    $c := b$;

    $k^{(l)}_{\min} := k^{(l-1)}_{\min} - 1$;

  else

    $c := a$;

    $k^{(l)}_{\min} := k^{(l-1)}_{\min}$;

  end(if)

  $P^{(l)}_{i+\frac{1}{2}}(\alpha) := P^{(l-1)}_{i+\frac{1}{2}}(\alpha) + c\prod_{i=k^{(l-1)}_{\min}}^{k^{(l-1)}_{\min}+l-1}(\alpha - \alpha_i)$;

end(for)

stop *with result* $f_i^+ = \frac{d}{d\alpha}P^{(r)}_{i+\frac{1}{2}}(\alpha_i)$.

Similarly, the r-th order left-biased approximation f_i^- to the derivative can be calculated by constructing $P^{(r)}_{i-\frac{1}{2}}(\alpha)$ associated with the interval $[\alpha_{i-1}, \alpha_i]$. As a special case, the algorithm yields the first order approximation (2.12) when $r = 1$. As a higher order example, the above algorithm with $r = 3$ chooses one of the stencils illustrated in Figure 3.1 to calculate f_i^+.

Based on (2.11) and Algorithm 3.1, the following algorithm describes a r-th order numerical scheme for the calculation of MEPs.

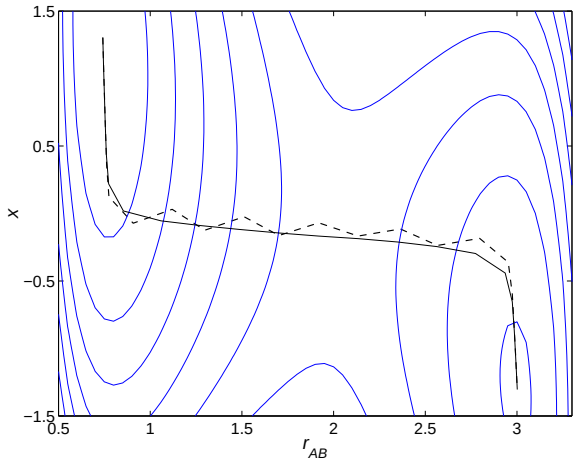

FIG. 4.1. *The contour plot of the energy surface used in Example 1 superposed by the MEP (solid line). The dashed line is the path obtained by the string method in which the tangent vectors are approximated by central finite differences. The kinks in the path show the numerical instabilities.*

ALGORITHM 3.2. *[String method for the MEP]*

Given discretized initial path $\{\varphi_i^{(0)}, i = 0, 1, \cdots, N\}$ *and tolerances* $0 < TOL_1 < 1$, $TOL_2 > 0$*;*

for $k = 1, 2, \cdots$

Calculate the tangent vectors based on (2.11) and Algorithm 3.1;

Integrate (2.9) using standard ODE solver, e.g. forward Euler or TVD Runge-Kuta, to obtain the new path $\{\varphi_i^{(k)}, i = 1, 2, \cdots, N\}$ *at* $t = t_k$*;*

if $\min_i ||\varphi_i^{(k)} - \varphi_{i+1}^{(k)}|| \leq TOL_1 \max_i ||\varphi_i^{(k)} - \varphi_{i+1}^{(k)}||$

Reparameterize $\{\varphi_i^{(k)}, i = 1, 2, \cdots, N\}$ *by polynomial interpolation;*

end(if)

if $||\nabla^{\perp} V(\varphi^{(k)})|| \leq TOL_2$

stop *with the MEP* $\varphi^{(k)}$*;*

end(if)

end(for)

In Algorithm 3.2, the string is parameterized by normalized arc-length or potential weighted arc-length depending on the definition of the norm $||\cdot||$. TOL_1 is a parameter that controls the distribution of points along the string.

4. Numerical Examples

Example 1 (LEPS potential coupled with harmonic oscillator). We consider the system involving four atoms A, B, C and D which are confined in a line. Atom B can form a chemical bond with either A or C, and interact with the fourth atom D in a harmonic way. The form of the potential can be found in [8]. A contour plot of the potential surface is given in Fig 4.1.

Fig 4.1 illustrates the numerical instabilities when the tangent vector is approximated by central finite differences. We start with the linear interpolation between the two minima, and use the forward Euler scheme to integrate (2.9). The path eventually forms kinks which oscillate back and forth, and as a result, the path fails to converge to the MEP.

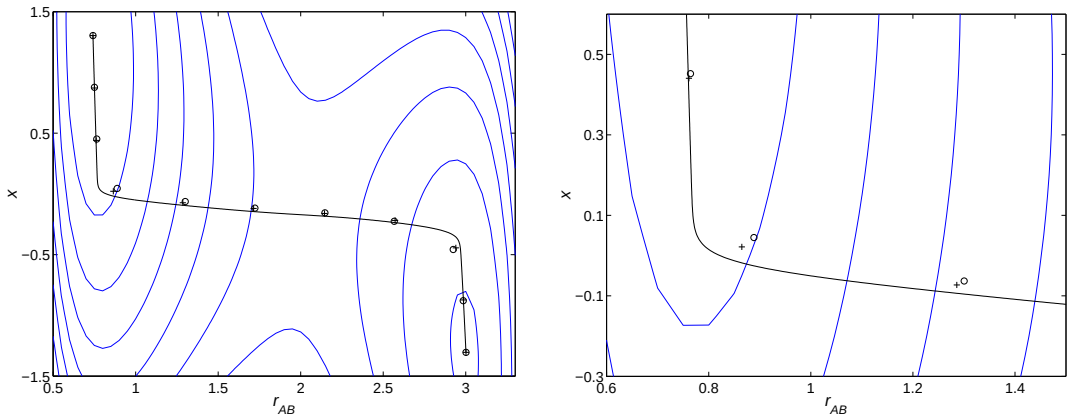

FIG. 4.2. *The numerical results in Example 1 by the scheme described in Algorithm 3.2.* $'\circ'$ *and* $'+'$ *correspond to* $r = 1$ *and* $r = 3$ *respectively. Both schemes are stable and converge to the MEP (solid line) nicely, while with* $r = 3$ *the scheme yields higher order accuracy.*

	$r = 1$		$r = 3$	
	L_∞ error (order)	L_2 error (order)	L_∞ error (order)	L_2 error (order)
10	6.71×10^{-2} (-)	2.40×10^{-2} (-)	3.75×10^{-2} (-)	1.70×10^{-2} (-)
20	3.10×10^{-2} (1.11)	6.64×10^{-3} (1.85)	1.77×10^{-2} (1.08)	6.11×10^{-3} (1.48)
40	1.97×10^{-2} (0.65)	3.31×10^{-3} (1.00)	6.30×10^{-3} (1.49)	6.88×10^{-4} (3.15)
80	1.40×10^{-2} (0.49)	1.65×10^{-3} (1.00)	3.54×10^{-3} (0.83)	1.81×10^{-4} (1.93)
160	7.47×10^{-3} (0.91)	8.10×10^{-4} (1.03)	7.08×10^{-4} (2.32)	3.37×10^{-5} (2.42)
320	3.85×10^{-3} (0.96)	3.99×10^{-4} (1.02)	1.13×10^{-4} (2.65)	4.51×10^{-6} (2.90)

TABLE 4.1. *The* L_∞ *and* L_2 *errors in Example 1 using Algorithm 3.2 with* $r = 1$ *and* $r = 3$ *respectively. The numbers in the parenthesis indicate the orders of accuracy. The results demonstrate that with* $r = 1$*, the scheme is first order accurate, while with* $r = 3$*, it achieves roughly third order accuracy.*

In Fig 4.2, we show the results obtained by the numerical scheme described in Algorithm 3.2. The solid line is the exact MEP, and the discrete points are the numerical results corresponding to $r = 1$ and $r = 3$ respectively. In both situations, the scheme is stable and converges to the MEP nicely, while with $r = 3$ it achieves higher order accuracy, as easily seen in the region where the path is curved.

In Table 4.1, we print out the L_∞ and L_2 errors of both schemes for various discretization points. The results demonstrate that with $r = 1$, the scheme is first order accurate, while with $r = 3$, it yields roughly third order accuracy.

Example 2 (Mueller potential). In this example, we applied Algorithm 3.2 to calculate the MEP in Mueller potential (see [10]). Mueller potential is invented as a nontrivial test example for reaction path algorithms. Again, we tested the algorithm with $r = 1$ and $r = 3$, and the numerical results are displayed in Fig 4.3. From Fig 4.3 we can clearly see the improvement on the accuracy by higher order schemes. The numerical errors and orders of accuracy are shown in Table 4.2. Again, the results show that the scheme is first order accurate with $r = 1$, while 1+ achieves third order accuracy with $r = 3$.

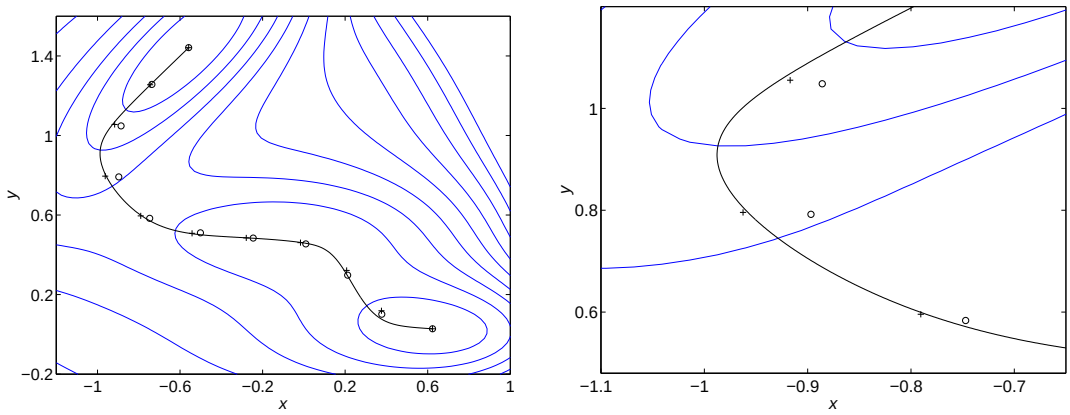

FIG. 4.3. *The numerical results in Example 2 by Algorithm 3.2. 'o' and '+' correspond to the schemes with $r = 1$ and $r = 3$ respectively. The solid line is the exact MEP. The results show that with $r = 3$, the scheme improves the accuracy significantly.*

	$r = 1$		$r = 3$	
	L_∞ error (order)	L_2 error (order)	L_∞ error (order)	L_2 error (order)
10	$5.19 \times 10^{-2}(-)$	$1.55 \times 10^{-2}(-)$	3.42×10^{-2} (-)	7.04×10^{-3} (-)
20	3.57×10^{-2} (0.54)	8.32×10^{-3} (0.90)	4.71×10^{-3} (2.86)	1.02×10^{-3} (2.79)
40	1.72×10^{-2} (1.05)	3.47×10^{-3} (1.26)	1.26×10^{-3} (1.90)	2.25×10^{-4} (2.18)
80	8.96×10^{-3} (0.94)	1.75×10^{-3} (0.99)	2.39×10^{-4} (2.40)	3.43×10^{-5} (2.71)
160	4.53×10^{-3} (0.98)	8.34×10^{-4} (1.07)	2.84×10^{-5} (3.07)	4.54×10^{-6} (2.92)
320	2.30×10^{-3} (0.98)	4.06×10^{-4} (1.04)	3.50×10^{-6} (3.02)	6.55×10^{-7} (2.79)

TABLE 4.2. *The L_∞ and L_2 errors in Example 2 using Algorithm 3.2 with $r = 1$ and $r = 3$ respectively. The numbers in the parenthesis indicate the order of accuracy. With $r = 1$, the scheme is first order accurate, while with $r = 3$ it achieves roughly third order accuracy.*

5. Conclusion

We have presented a numerical scheme for finding the minimum energy paths in metastable systems. The construction of the numerical scheme is based on the idea of the upwind scheme and the ENO scheme. The numerical experiments demonstrate that the scheme is stable and achieves higher order accuracy. A weighted ENO scheme which has the same stencil nodes as the ENO scheme but achieves even higher order accuracy can be implemented as well.

Acknowledgment. The author is grateful to Eric Vanden-Eijnden, Bob Kohn and especially Weinan E and Li-Tien Cheng for stimulating discussions. This work was supported in part by a NSF grant DMS-9729992.

REFERENCES

[1] P.G. Bolhuis, D. Chandler, C. Dellago, and P. Geissler, *Transition path sampling: throwing ropes over mountain passes, in the dark.* Ann. Rev. of Phys. Chem., 59:291, 2002.

[2] W. E, W. Ren, and E. Vanden-Eijnden, *String method for the study of rare events.* Phys. Rev. B., 66:052301, 2002.

[3] W. E, W. Ren, and E. Vanden-Eijnden, *Probing multi-scale energy landscapes using the string method*. submitted to Phys. Rev. Lett.
[4] W. E, W. Ren, and E. Vanden-Eijnden, *Energy landscape and thermally activated switching of submicron-sized ferromagnetic elements*. J. Appl. Phys., 93:2275–2282, 2003.
[5] M.I. Freidlin and A.D. Wentzell, *Random perturbations of dynamical systems*. 2nd ed. Springer, New York, 1998
[6] G. Henkelman and H. Jónsson, *Improved tangent estimate in the nudged elastic band method for finding minimum energy paths and saddle points*. J. Chem. Phys., 113:9978, 2000.
[7] I.V. Ionova and E.A. Carter, *Ridge method for finding saddle points on potential energy surfaces*. J. Chem. Phys., 98:6377, 1993.
[8] H. Jónsson, G. Mills, and K. W.Jacobsen, *Nudged elastic band method for finding minimum energy paths of transitions*. Classical and Quantum Dynamics in Condensed Phase Simulations, ed. B.J. Berne, G. Ciccotti, and D.F. Coker, World Scientific, 1998.
[9] G.S. Jiang and D. Peng, *Weighted ENO schemes for hamilton-jacobi equations*. SIAM J. Sci. Comput., 21:2126–2143, 2000.
[10] R. Olender and R. Elber, *Calculation of classical trajectories with a very large time step: Formalism and numerical examples*. J. Chem. Phys., 105:9299, 1996.
[11] S. Osher and C.W. Shu, *High-order essentially nonoscillatory schemes for hamilton-jacobi equations*. J. Numer. Anal., 28:907–922, 1991.
[12] W. Ren, *Numerical methods for the Study of Energy Landscapes and rare events*. PhD thesis, New York University, 2002.